Chinese Chemical Letters 35 (2024) 109143

Contents lists available at ScienceDirect

Chinese Chemical Letters

journal homepage: www.elsevier.com/locate/cclet

Water molecules regulation for reversible Zn anode in aqueous zinc ion battery: Mini-review

Jie Zhou[a], Quanyu Li[a], Xiaomeng Hu[a], Weifeng Wei[a], Xiaobo Ji[b], Guichao Kuang[a], Liangjun Zhou[a,*], Libao Chen[a], Yuejiao Chen[a,*]

[a] State Key Laboratory of Powder Metallurgy, Central South University, Changsha 410083, China
[b] College of Chemistry and Chemical Engineering, Central South University, Changsha 410083, China

ARTICLE INFO

Article history:
Received 17 July 2023
Revised 9 August 2023
Accepted 22 September 2023
Available online 23 September 2023

Keywords:
Electrolyte engineering
Aqueous zinc ion battery
Zinc metal anode
Dendrite suppression
Mildly acidic electrolyte

ABSTRACT

With the low cost, excellent safety and high theoretical specific capacity, aqueous zinc-ion batteries (AZIBs) are considered as a potential rival for lithium-ion batteries to promote the sustainable development of large-scale energy storage technologies. However, the notorious Zn dendrites and low Coulombic efficiency (CE) limit further development of AZIBs, due to the unstable electrochemical deposition/stripping behavior of Zn anode in aqueous zinc ion electrolytes. In this review, critical issues and advances are summarized in electrolyte engineering strategies. These strategies are focused on active water molecules during electrochemical process, including high-concentration electrolytes, ionic liquids, gel-polymer electrolytes and functional additives. With suppressed active water molecules, the solvation and de-solvation behavior of Zn^{2+} can be regulated, thereby modulating the electrochemical performance of Zn anode. Finally, the inherent problems of these strategies are discussed, and some promising directions are provided on electrolytes engineering for high performance Zn anode in AZIBs.

1. Introduction

With the increasing demand in the energy storage market and environmental concerns, designing sustainable devices for environmentally friendly, renewable energy storage is crucial. Wind, solar and tidal energy provide some relief, but they are unstable and unpredictable. The lithium-ion batteries have gained the most share of the energy storage market in the latest 30 years because of the superior energy density and long cycle life, but the concerns about safety and expensive raw materials have limited the further application [1–4]. Distinguishing from lithium-ion batteries that match organic electrolytes, aqueous zinc-ion batteries have garnered extensive attention since 2018 because of their inherent safety, abundant raw materials and the high theoretical volumetric capacity of Zn (5855 mAh/cm^3 or 820 mAh/g) [5,6]. However, the significant development of aqueous zinc-ion batteries is still hindered by the limited reversibility of the zinc anode and low Coulombic efficiency (CE), primarily caused by the instability of the zinc anode in aqueous environments [7–9].

When zinc anode surfaces come into contact with active water molecules, microscopic voltaic cells are formed on the surface, thus the corrosion occurs even without applied electric field, while hydrogen gas is generated through the dissociation of water [10]. Limited by the intrinsic water splitting reactions including oxygen evolution reaction (OER) and hydrogen evolution reaction (HER), the theoretical electrochemical stability windows (ESW) of aqueous batteries are narrow (1.23 V) [11]. Besides the formation of by-products that can cause passivation of the zinc anode and consumption of electrolytes. The uneven electric field distribution on the surface of zinc anode is caused by the above problems, thus resulting in notorious zinc dendrites. During the later Zn stripping/plating process, the fracture of zinc dendrites to form so-called “dead” zinc, leading to low Coulombic efficiency and capacity loss [12]. Unlike organic-based battery systems, aqueous batteries also need to consider their pH value of electrolytes. Under different pH conditions, aqueous zinc-ion batteries have different challenges and anodic reaction mechanisms [13]. In alkaline conditions, dendrites growth and OER dominate, Zn anode can transfer to the water-soluble $Zn(OH)_4^{2-}$. After accumulating to a certain extent, the formation of conductively poor by-products, such as zinc oxide and zinc hydroxide, leads to passivation of the zinc electrode. Under acidic conditions, the corrosion and hydrogen evolution reaction (HER) need to be overcome, with passivation being

---

* Corresponding authors.
E-mail addresses: alexander-zhou@csu.edu.cn (L. Zhou), cyj.strive@csu.edu.cn (Y. Chen).

https://doi.org/10.1016/j.cclet.2023.109143

alleviated [14]. Different from strongly acid and alkali electrolyte with more inferior morphological instability of Zn anode, the employment of mildly acidic (pH 3–7) aqueous electrolytes plays a vital role during the critical phase of energy transition. Since it possesses intrinsic safety, recyclability and high economic benefits, making it highly applicable in energy storage systems [15,16].

To obtain high performance Zn anode in aqueous zinc-ion batteries, it is vital and convenient to design the electrolyte composition, in this review, the issues about corrosion and dendrites on the Zn anode are clarified, and we timely summarize the electrolyte design engineering *via* the regulation of active water molecules for Zn anode protection. We will divide electrolyte strategies into the following categories: high-concentration electrolytes, ionic liquids, gel-polymer electrolytes and functional additives. The strategies provided also can applied in other Zn-based energy storage systems, such as Zn-air batteries or zinc ion hybrid capacitor. Lastly, the verified electrolyte regulation mechanisms and promising perspectives on potential future research are outlined. We hope that this review can provide a comprehensive reference to effectively design electrolyte for high performance aqueous zinc-ion batteries and other aqueous ion batteries, such as aluminum, magnesium, and calcium ion batteries.

2. Corrosion and dendrites

Currently, commercial zinc foil is commonly used as the anode in AZIBs. However, the zinc anode is unstable in aqueous electrolytes due to corrosion and dendrites related to active water molecules [17,18]. Both chemical and electrochemical corrosion issues exist. Chemical corrosion dominates during resting state; electrochemical corrosion is the main problem during cycling state due to the repeated Zn deposition/stripping processes [19]. The zinc ions tend to coordinate with water molecules in the aqueous electrolyte environment, and the process of solvated zinc-ion deposition can be roughly divided into the following steps: (1) Diffusion of solvated Zn^{2+}; (2) de-solvation of Zn^{2+}; (3) charge transfer; and (4) nucleation and growth [8].

Because of the reduction potential (−0.76 V *vs.* SHE) of Zn metal [20], the H^+ ions from polarized water molecules will be reduced to hydrogen during Zn^{2+} deposition process, thermodynamically. There are two sources of polarized water molecules in contact with the zinc anode. One is the bulk water molecules in electrolyte, and the other is the de-solvated water molecules of the carrier Zn^{2+}. The increase in hydroxide (-OH) concentration caused by HER will change the pH value of electrolyte, and convective disturbance of hydrogen bubbles impacts the voltage stability [21]. The continuous H_2 evolution will exacerbate the inhomogeneity of Zn^{2+} flux reaching the surface of zinc matrix, leading to an increase of the concentration polarization near the interface. The protruding Zn caused by non-uniform deposition has a higher curvature and therefore produces a higher electric field due to the 'tip effect', Zn^{2+} are preferentially nucleate in and 2D diffuse to these active sites [22], which promotes the rapid growth of Zn dendrites and worsens the inhomogeneity of Zn anodes. In addition, dendrites in turn promote corrosion by increasing the reaction surface area [5]. Since these problems do not exist in isolation, but are closely related to each other, it is necessary to focus on the core of these problems when designing optimized electrolyte formulations (Fig. 1). The water solvent provides fast charge transfer kinetics, due to the intrinsic high polarity of water molecules and small carriers size in aqueous electrolyte. Simultaneously, divalent nature of Zn^{2+} enhance the electronic interactions with charged skeleton, thus inhibit diffusion process, fast ion migration is facilitated by the shielding effect of water molecules on Zn^{2+} ions [17]. But aforementioned side reactions are directly related to active water molecules. The water in the electrolyte molecules is a double-edged sword. Therefore, in the application of electrolyte engineering to stabilize zinc-ion batteries, attention should be paid to the regulation of water molecules.

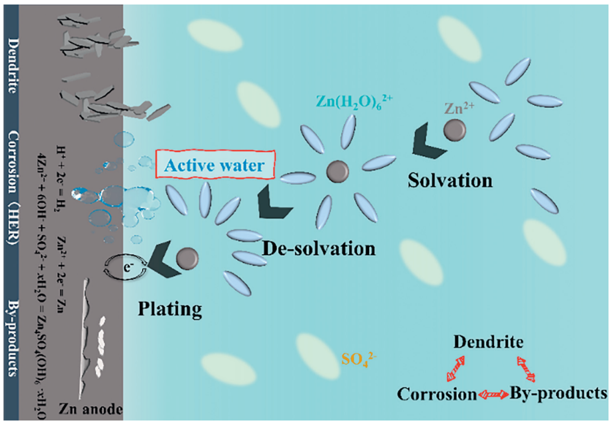

Fig. 1. Schematic diagram of the interfacial side reactions on the zinc anode in mildly acidic electrolytes.

3. Electrolyte design engineering

To suppress the issues caused by water molecules while maintaining the inherent safety and high conductivity of aqueous electrolytes, it is desirable to keep the water molecules in an electrochemically stable state. This can be achieved by constructing a hydrophobic region on the zinc metal surface to achieve anodic protection at the interface, as well as by inhibiting the activity of water molecules (suppressing the polarization of free water molecules on the zinc anode surface). Researches regulating the Zn anode/electrolyte interface currently focus on composition and structure design, surface modification of Zn anode and electrolyte regulation [15,23,24]. Both of the first two operations are complicated, and the processing time of surface modification is much longer. The interface state between Zn anode and the electrolyte significantly depends on the electrolyte system since the electrolyte acts as a communication channel between the cathode and anode. Therefore, systematic research on electrolyte regulation engineering is necessary.

Adjusting the electrolyte is a convenient strategy that allows for dynamic regulation of the interface. In neutral or mildly acidic systems, the corrosion issue of the zinc anode is more severe compared to alkaline systems [17], this is due to the lack of passivation effect of amphoteric zinc oxide (ZnO). Currently, the commercial electrolytes used in aqueous zinc-ion batteries are mildly acidic, such as zinc sulfate ($ZnSO_4$) and zinc trifluoromethanesulfonate [$Zn(OTf)_2$], which have ultra-high ionic conductivity [25]. For large-scale commercialization, it is necessary to consider further modifications to the zinc sulfate electrolyte (Fig. 2). One strategy for regulating aqueous electrolytes is to reduce the quantity of water molecules, which includes the use of high-concentration electrolytes [26], ionic liquids [27–29] and gel polymer electrolytes [30–37]. Another approach involves the use of functional additives in the existing aqueous electrolyte to displace or occupy the solvation shell of zinc-ions, thus blocking water-induced corrosion on the zinc anode surface [38–44]. The addition of additives facilitates the de-solvation process of zinc-ions and prevents direct contact between active water and the zinc anode surface, which is an economically effective method of control. The corresponding water molecules regulation strategies in electrolyte are shown in Fig. 2 [27,28,45-49]. In the next part, we will discuss the advantages and disadvantages of these electrolyte modification strategies in detail.

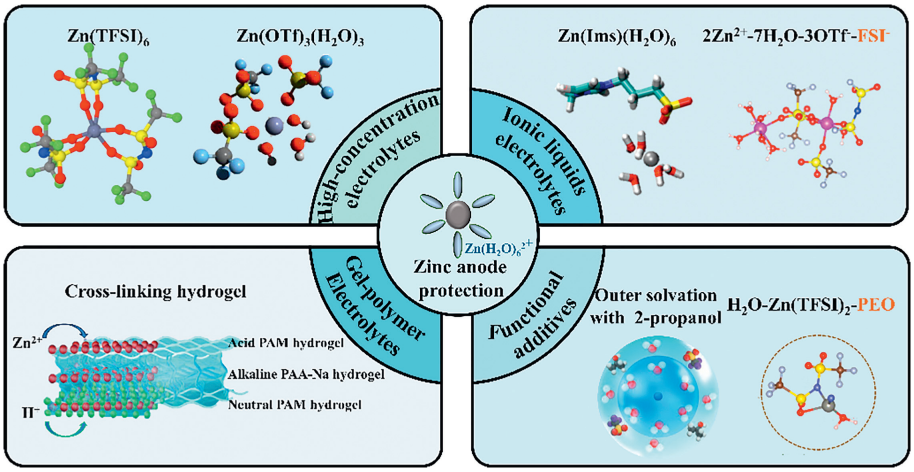

Fig. 2. Overview of the electrolyte engineering for zinc anode protection with suppressed water molecules. Reproduced with permission [27]. Copyright 2022, Royal Society of Chemistry. Reproduced with permission [28]. Copyright 2023, John Wiley and Sons. Reproduced with permission [45]. Copyright 2022, American Chemical Society. Reproduced with permission [46]. Copyright 2018, Springer Nature. Reproduced with permission [47]. Copyright 2021, John Wiley and Sons. Reproduced with permission [48]. Copyright 2021, Elsevier. Reproduced with permission [49]. Copyright 2022, John Wiley and Sons.

3.1. High-concentration electrolytes

When zinc salts dissolve in water, water molecules spontaneously coordinate with zinc-ions to form hydrated zinc-ions $[Zn(H_2O)_6{}^{2+}]$, in a commercial electrolyte, water molecules are relatively abundant. Zinc-ions attract six regularly arranged water molecules through a strong electrostatic potential field, while the arrangement of outer shell water molecules is partially ordered with an indefinite number. Therefore, the strategy of increasing solute concentration to expel water molecules from the solvation shell has emerged. As the concentration of electrolyte salts increases, the number of solvent water molecules decreases, and the distance between the cations and anions shortens, leading to the formation of what is known as water-in-salt electrolytes (WISEs). In highly concentrated states, cations and anions exist in pairs, resembling the characteristics of ionic liquids. Detailed discussions regarding ionic liquids will be presented in the next subsection. The effectiveness of artificial solid electrolyte interface layers (SEI) is demonstrated in metal batteries (magnesium metal batteries, sodium metal batteries and lithium metal batteries) [2,45,46]. Tens of anions and cations can induce the *in-situ* formation of a SEI, which stably protect the Zn anode during electrochemical stripping/plating, achieving corrosion inhibition and regulating cyclic stability. Particularly, highly concentrated electrolytes can effectively widen the narrow voltage window (1.23 V) limited by solvent water [47], there is potential to achieve higher energy density in zinc-based batteries.

The salt concentration from 'dilute' to 'super-concentrated' leads to a stepwise change in the state of zinc ions and salt existence (Fig. 3a) [18], and the electrochemical stability window (ESW) of aqueous electrolytes with different concentrations (Fig. 3b) [11]. The high-concentration enhance the coordination number of anions in the inner solvation shell of Zn^{2+}, but the maximum concentration is limited by solubility. Typically used zinc salts like $ZnSO_4$, $Zn(TFSI)_2$, and $ZnCl_2$ have low solubility in aqueous solutions (typically below 21−32 mol/kg). Gao *et al.* achieved a high concentration of up to 75 mol/kg by adding water–salt oligomers. As the salt concentration increases, the water content of the solvation shell surrounding zinc ions decreases sharply (Fig. 3c) [26]. Moreover, with additional chlorine salts and dimethyl carbonate in concentrated $ZnCl_2$ electrolyte, the formation of a double-layered organic/inorganic composite SEI stably protect the Zn anode (Fig. 3d) [48]. The obtained SEI enabled stable cycling of a pouch cell with a $VOPO_4{\cdot}2H_2O$ cathode under practical conditions for 500 cycles, providing an energy density of 100 Wh/kg. Wang *et al.* [49] achieved dendrite-free Zn stripping/plating with nearly 100% Coulombic efficiency using a high-concentration LiTFSI/$Zn(TFSI)_2$ saltwater electrolyte (Figs. 3e and f), TFSI, bis(trifluoromethanesulfonyl)imide). Of note, the compromise between high stable voltage windows and the rate performance should have to be taken into account when committed to increasing salt concentration, the ultra-high electrolyte concentration posed challenges such as high viscosity and low ionic conductivity. Localized high-concentration electrolytes for lithium-ion batteries have gained extensive attention, and it is believed that they also provide insights for concentration regulation in zinc-based battery electrolytes. There is a recent research has focused on controlling the concentration gradient in electrolytes [50], thus mitigating the side effects dominated by the high activity of water molecules and regulate the kinetics of needed interfacial reactions.

Currently, high-concentration electrolytes are mostly prepared using fluorine-containing salts, which pose significant challenges in terms of cost and environmental sustainability [18,47,51]. Moreover, they are likely to sacrifice the kinetics of the carrier. In order to achieve large-scale commercial applications, it is not a long-term solution to rely solely on the stacking of high-concentration salt. In the future, researches on high-concentration electrolytes still needs to address issues related to economic viability and charge transfer kinetics.

3.2. Ionic liquids electrolytes

Ionic liquids are molten salts with low melting points (below 100 °C) that consist solely of ions. They are characterized by their non-volatility, non-flammability, and a wide range of selectable components. Furthermore, they exhibit excellent stability in terms of their properties [52]. Ionic liquids exist in a neutral ion pair state [27], which effectively stabilizes the stripping/plating behavior of Zn^{2+} and expands the electrochemical stable window, but the high cost limits further large-scale application. Pure ionic liquids used as electrolytes suffer from high viscosity, which hinders ion diffusion kinetics [53]. However, if introduced as additives to commercial electrolytes with a suitable ratio, the high conductivity and wide stable voltage window of ionic liquids can be achieved while retaining the high fluidity and interface compatibility of the commercial electrolyte [54]. Of note, selecting a aqueous

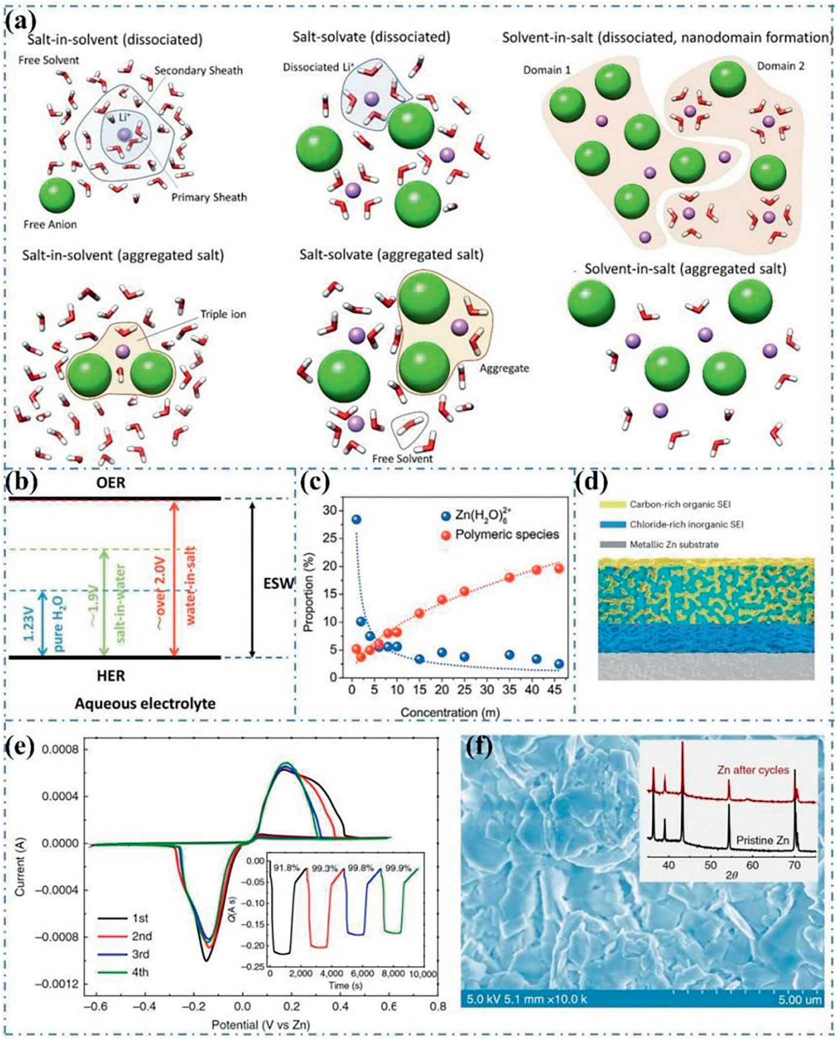

Fig. 3. (a) Diagram illustrating different concentrations into three regimes for dissociating and aggregating salts. Reproduced with permission [18]. Copyright 2022, Elsevier. (b) The ESW of aqueous electrolytes at various concentrations. Reproduced with permission [11]. Copyright 2022, John Wiley and Sons. (c) Trends in the variations of $Zn(H_2O)_6{}^{2+}$ and polymeric species content in electrolytes ranging from 1 mol/L to 46 mol/L. Reproduced with permission [26]. Copyright 2021, John Wiley and Sons. (d) Schematic illustrating the structure of dual-layer SEI in the Zn anode with electrolyte of 30 mol/L $ZnCl_2 + 5$ mol/L LiCl. Reproduced with permission [48]. Copyright 2023, Springer Nature. (e) Cyclic voltammogram illustrating the process of Zn stripping/plating in a three-electrode cell. Inset: Chronocoulometry curves. (f) Scanning electron microscope (SEM) image of the Zn anode after undergoing 500 stripping/plating cycles in 1 mol/L $Zn(TFSI)_2 + 20$ mol/L LiTFSI electrolyte. Inset: X-ray diffraction (XRD) pattern. Reproduced with permission [49]. Copyright 2018, Springer Nature.

basic electrolyte with suitable ionic liquid additive components can construct a stable SEI and improve the reversibility of zinc anodes [55].

Chen *et al.* [27] constructed an adaptive inner Helmholtz layer at the zinc anode with zwitterionic liquid additives, 3-(1-methylimidazole)propanesulfonate (ImS) (Fig. 4a), to induce homogenous Zn^{2+} flux at the interface and gain high-voltage characteristics (Fig. 4b). Even in the state of high zinc utilization ratio (85%), the Zn anode cycling performance was improved by 35 times compared to a commercial aqueous electrolyte (2 mol/L $ZnSO_4$). This type of ionic liquid also simultaneously regulated the double-layer structure at the cathode, inferior interfacial of both Zn anode and the cathode being synchronously regulating should be the key during stripping/plating cycles. Yu *et al.* [28] added 1-ethyl-3-methylimidazolium bis(fluorosulfonyl)amide (EmimFSI), which is immiscible with water, to a aqueous $Zn(OTf)_2$ system to encapsulate zinc ions coordinated with active water molecules (Fig. 4h), this effectively blocked parasitic reactions triggered by active water molecules. The additive effect of this composition strategy can enhance overall performance especially for high-voltage zinc ion batteries. Additionally, research has shown that a small amount of water molecules can enhance the ion conductivity of ionic liquid electrolytes by providing lubrication, while the ionic liquid network restricts the activity of water molecules (Fig. 4c) [56]. Previous researches have demonstrated that adding grafting ionic liquids to solid or *quasi*-solid electrolytes can have synergistic effect. For example, compared to Zn/Zn^{2+}, water only exhibited an electrochemical stability window of −0.05 V to 1.7 V. When $EMIMBF_4$ was added, the stability window was extended to −0.75 V to 2.8 V (Fig. 4d) [57]. The ionic liquids additive endows the low vapor pressure of ionic liquids provides excellent safety and physical-chemical stability to the AZIBs (Figs. 4e and i) [57,58], highlighting the parallelism of electrolyte pathways. Special ionic liquid cations, such as 1–butyl–3-methylimidazolium cation ($BMIm^+$ ion), have the function of inducing (002) zinc deposition (Figs. 4f and g) [59], which provides inspiration for designing electrolyte components to restructure the preferred texture of Zn anodes.

At present, the research on the influence law of anion and cation needs to be further systematized and comprehensive. The design of ionic liquids, which have the ability to optimize the electrolyte/electrode interface, needs to be based on the comprehen-

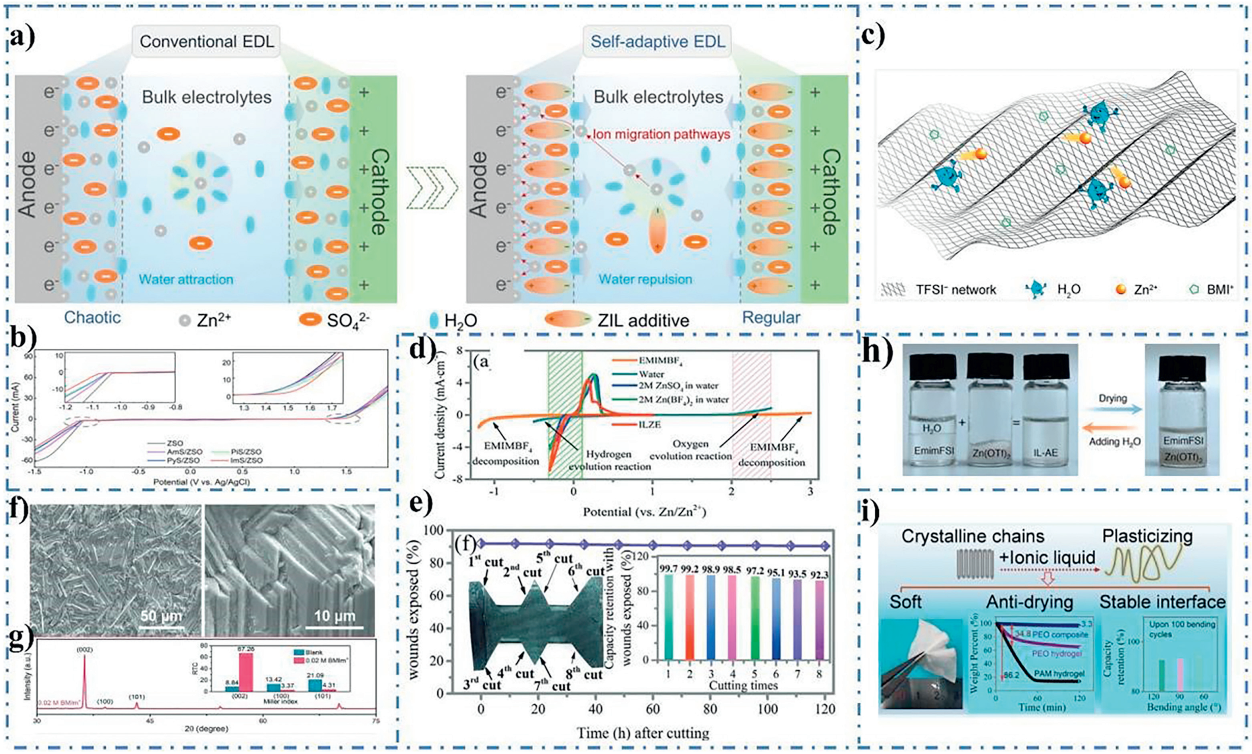

Fig. 4. (a) Mechanism diagram of a self-adaptive electric double layer construction in ionic liquid additive electrolyte. (b) The ESW of basic electrolyte a series of zwitterionic ionic liquids additives in the electrolyte. Reproduced with permission [27]. Copyright 2022, Royal Society of Chemistry. (c) Schematic diagram of water locking network structure constructed by ionic liquids. Reproduced with permission [56]. Copyright 2023, American Chemical Society. (d) The ESW of basic electrolyte and EMIMBF$_4$ ionic liquids additives electrolyte. (e) Capacity retention ratio of all-solid-state batteries with EMIMBF$_4$ ionic liquid additives in the electrolyte under varying cutting times. Reproduced with permission [57]. Copyright 2020, John Wiley and Sons. (f) SEM images and (g) XRD of cycled Zn anodes morphology with 0.02 m BMIm$^+$ additives electrolyte under 5 mA/cm^2. Inset: Corresponding texture parameters of Zn anodes. Reproduced with permission [59]. Copyright 2022, John Wiley and Sons. (h) Digital images of the transformation of the initially immiscible H$_2$O-EmimFSI binary system into a homogeneous solution through the incorporation of Zn(OTf)$_2$, demonstrating ionic liquid acting as "water pocket". Reproduced with permission [28]. Copyright 2023, John Wiley and Sons. (i) Schematic illustrating ionic liquids optimized gel-polymer electrolyte for anti-drying and stable interface. Reproduced with permission [58]. Copyright 2022, American Chemical Society.

sive consideration of the role of anions and cations in the reversible Zn deposition/stripping and the inhibition of HER. Due to the wide variety of ionic liquids, it is flexible and efficient to disassemble them into pairs of functional ions, and more kinds of ionic liquids need to be applied to ZIBs. The use of ionic liquid as an additive can alleviate the problem of its expensive price to a certain extent.

3.3. Gel-polymer electrolytes

Solid-state/*quasi*-solid-state electrolytes are ideal electrolytes for flexible zinc-ion energy storage devices due to their high safety, flexibility and mechanical properties [60]. Reduced water molecule content and polymerized electrolyte solved the most of problems of electrolyte leakage and water splitting, which are fatal in large-scale application of AZIBs. In contrast to liquid electrolytes, highly crystalline solid-state/*quasi*-solid-state electrolytes have substantially worse motion properties [53], gel polymer electrolytes are *quasi*-solid-state electrolytes obtained by crosslinking polymers with zinc salts while retaining a small amount of water molecules; water molecules play a role in lubrication and reducing the energy barrier of charge diffusion. However, gel-polymer electrolytes are subject to low ion conductivity at room temperature and interface wetting issues hitherto [57,61]. Traditional methods for preparing gel polymer electrolytes include phase transition, solvent casting, and *in-situ* polymerization [62]. Gel polymer electrolytes that possess high ion conductivity and low electronic conductivity have the potential to serve as both electrolytes and separators in batteries [63], thus enhancing the energy density of entire battery system.

Luo *et al.* developed a polyzwitterionic hydrogel electrolyte (PZHE) with polar N and O groups, which immobilizes water molecules within the polymer framework. The polar groups effectively bind and retain water molecules [64]. Through *in-situ* optical microscopy observations, it was found that the Zn//Zn symmetric cell using PZHE exhibited significantly suppressed HER during electrochemical cycling (Fig. 5a), the reversibility of the Zn anode was improved (lifespan of over 3500 h under 0.5 mA/cm^2), with a room temperature ion conductivity of 32 mS/cm and the Zn^{2+} migration number of 0.656. Otherwise, the gel polymer can lift up the resting performance with suppressed chemical corrosion, Zhou *et al.* used tannic acid-modified sodium alginate to obtain a hydrogel with carboxyl groups and phenolic hydroxyl groups, which interact with Zn^{2+} ions [65]. Specifically, the zinc anode and its matched cathode have conflicting requirements for water molecules. In the zinc anode, corrosion can be suppressed by reducing the number of water molecules, while most cathodes require co-intercalation of protons and Zn^{2+} to achieve high capacity and high rate capability [66]. The synergies of reduced water content and zinc-philic ligand leads to uniform zinc deposition and improved shelf performance (Fig. 5d). The improved reversibility of the zinc anode was also confirmed in a Zn//Cu asymmetric cell (Fig. 5e) [63]. The gel-polymer electrolytes as well exhibit the potential in crossover fields. A hierarchical alginate hydrogel developed that simultaneously inhibits corrosion and byproducts (Fig. 5b). Through validation in the rabbit intestinal tract, the hydrogel demonstrated bio-

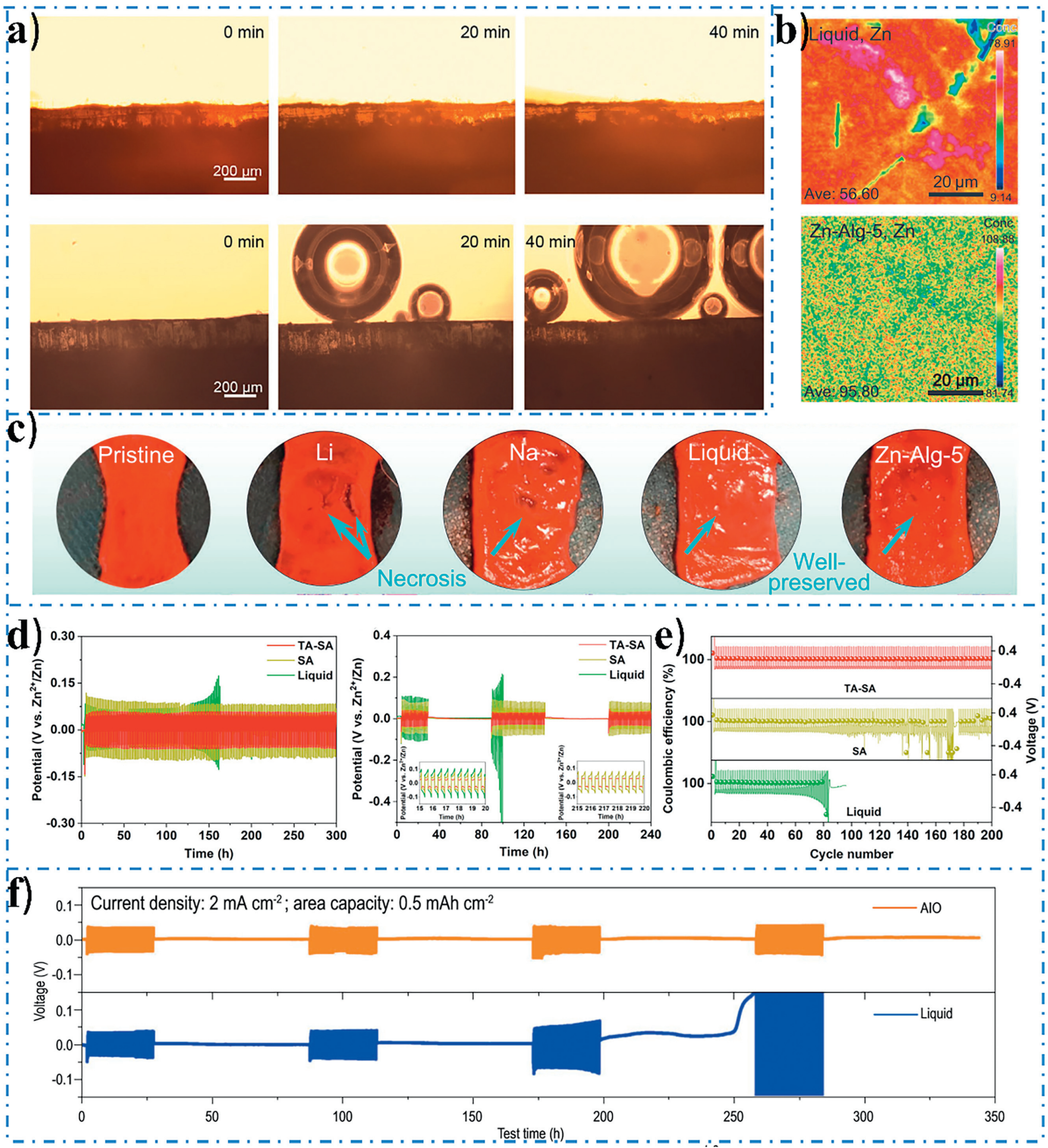

Fig. 5. (a) *In-situ* optical observation of Zn electroplating in Zn//Zn cells with poly[2-(methacryloyloxy)ethyl]dimethyl-(3-sulfopropyl) (PSBMA) hydrogel electrolyte and commercial liquid electrolyte. Reproduced with permission [64]. Copyright 2020, John Wiley and Sons. (b) The EPMA/WDS mapping of Zn elements intensity from Zn anode cycled with liquid electrolyte and alginate polymer electrolyte. (c) Optical photos of duodenal tissue in living rabbits after 6 h of storage of punched batteries with alginate polymer electrolyte. Reproduced with permission [67]. Copyright 2022, Oxford University Press. (d) Electrochemical performances of Zn//Zn symmetric cells with and without resting for 60 h under 1.13 mA/cm^2. (e) The Coulombic efficiency of the Zn//Cu asymmetric cells with tannic acid (TA) modified sodium alginate (SA) composite gel electrolyte, SA and liquid electrolyte. Reproduced with permission [65]. Copyright 2020, Elsevier. (f) Shelve performance of Zn//Zn symmetric cell with Sodium alginate gel electrolyte 'plating' and liquid electrolyte under 2 mA/cm^2. Reproduced with permission [68]. Copyright 2021, Oxford University Press.

compatibility for zinc battery applications (Fig. 5c) [67]. It exhibited excellent safety and enhanced the potential for zinc battery applications in wearable devices and biomedicine. The unique self-healing properties of hydrogels compared to liquid electrolytes can enhance the stability of the entire battery system (Fig. 5f) [68].

A very small amount of water molecular content inhibits the corresponding side reactions. Hydrogels with mechanical properties and certain ionic conductivity achieve a long-term stable cycle of the battery. Other commonly used hydrophilic matrix polymers such as poly(ethylene oxide) (PEO) [69], poly(vinylidene fluoride) (PVDF) [70], poly(vinyl alcohol) (PVA) [63,71,72], polyacrylamide (PAM) [73] and others regulate the zinc ion deposition behavior based on similar principles.

To enhance ion conductivity, the strategy can focus on lowering the crystallinity of the polymer electrolytes to achieve faster ion diffusion kinetics. Seeking the suitable ratio of polymer and zinc salt is also the key to improve the ionic conductivity in gel electrolyte applications. It is also need to consider the adaptability of the matrix polymer to zinc salts. Typical zinc salt cations like SO_4^{2-} and PO_4^{2-} based on the Hofmeister Series can induce salt out, leading to the disruption of the gel polymer's uniformity [74]. In order to regulate water molecules, Zhi *et al.* have developed a class of asymmetric electrolytes, where the zinc anode side consists of an inorganic solid-state electrolyte, and the cathode side is a hydrogel [61]. This work provides a design strategy for dendrite-free and near 100% CE solid/*quasi*-solid-state zinc ion batteries. In conclusion, hydrogel electrolytes can be used in unique application scenarios, such as wearable flexibility and biomedicine, but their large-scale application is severely constrained by their poor conductivity, inability to transport high current densities.

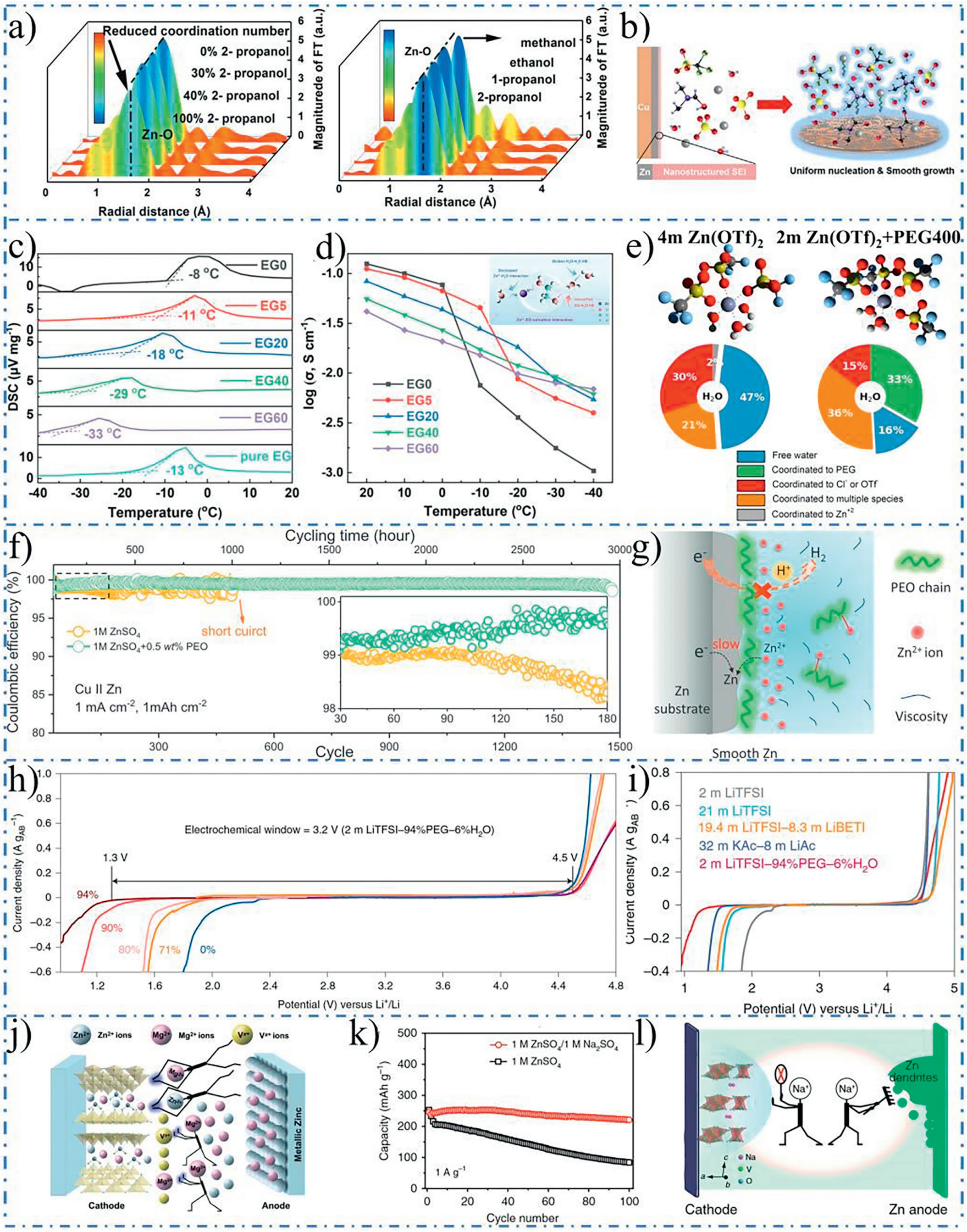

Fig. 6. (a) Study the solvation structure of Zn^{2+} with alcohol organic additives. synchrotron-radiation extended X-ray absorption fine structure (EXAFS) spectra for electrolytes. Reproduced with permission [98]. Copyright 2022, John Wiley and Sons. (b) Schematic diagram of the mechanism of SEI formation with *N*,*N*-dimethylformami-dium trifluoromethanesulfonate (DOTf) additives electrolytes. Reproduced with permission [120]. Copyright 2022, Elsevier. The performance of electrolytes at low temperatures by incorporating ethylene glycol additives: (c) Freezing point data from differential scanning calorimetry (DSC) curves and (d) the ionic conductivities of hybrid electrolytes at different temperatures. Inset: regulation mechanism. Reproduced with permission [100]. Copyright 2020, Royal Society of Chemistry. (e) Zn^{2+} Solvation structure and component content of 4 mol/L $Zn(OTf)_2$, and 4 mol/L $Zn(OTf)_2$ + PEG400 additives electrolyte. Reproduced with permission [107]. Copyright 2022, American Chemical Society. (f) Coulombic efficiency of Zn//Cu cells with and without long-chain polyethylene oxide (PEO) polymer additive electrolytes. (g) The Schematics of the mechanism PEO regulating Zn deposition behavior. Reproduced with permission [95]. Copyright 2020, John Wiley and Sons. (h) Linear sweep voltammetry tests of electrolyte with different concentrations of PEO and (i) different types electrolytes. Reproduced with permission [94]. Copyright 2020, Springer Nature. (j) Schematic diagram of the way $MgSO_4$ additive electrolyte alleviating the dissolution of cathode $MgxV_2O_5\cdot nH_2O$. Reproduced with permission [113]. Copyright 2020, Springer Nature. (k) Cycling performance of Zn//$NaV_3O_8\cdot 1.5H_2O$ (NVO) full batteries with and without Na_2SO_4 additives electrolytes. (l) Schematic diagram of the way Na_2SO_4 additives inhibits Zn dendrites and the breakdown of NVO nanobelts. Reproduced with permission [109]. Copyright 2018, Springer Nature.

3.4. Functional additives

Functional additives have been widely reported by researchers due to their excellent cost effectiveness. In the case of a trace amount of additive, the stability of the anode/electrolyte and cathode/electrolyte interface can be adjusted simultaneously, so the functional additives have spacious research prospects [75]. Significantly, some additives with a weakly solvating effect can regulate the solvation structure of Zn^{2+} and promote the de-solvation process [1,76], as well break the hydrogen-bonding network of water molecules simultaneously [77,78]. To achieve low-cost and high performance AZIBs, it is the strategy that shows the most promise compared to the others.

3.4.1. Organic additives

The investigation of organic additives mainly includes organic small molecules [76,79–91] and polymers [92–97]. The structure and composition of organic additives play a significant role in protecting the zinc anode, including factors such as molecular polarity, steric hindrance, and carbon chain length [38]. Organic additives with polar functional groups (such as N, O, and F, which possess strong electronegativity) can compete with water molecules in the solvation shell of Zn^{2+}. The coordinating ability of these additives can be regulated based on factors such as the number and distribution of polar functional groups, molecular size, and the number of donor sites. This allows for the design of solvent pathways and surface adsorption pathways [1].

Polar organic additives primarily function by preferentially adsorbing onto the zinc anode surface, forming a hydrophobic film that can resist the free water molecules flowing in the bulk phase. When hydrated Zn^{2+} arrives at the Zn anode while deposition process, the solvated water molecules also are expelled. A higher number of polar groups can better adsorb on the Zn anode surface; but may result in lower hydrogen evolution overpotential [62]. On the other hand, in the bulk phase, strongly coordinating additives can enter the solvation shell of zinc ions, altering the strong interaction between zinc ions and water molecules. Additionally, polar molecules can form bonds with water molecules, effectively binding them and limiting their activity. To achieve changes in solvation, it is generally necessary to consider parameters such as dielectric constant and molecular size. This is due to the combined consideration of coordination ability and steric hindrance effects. In general, larger solvation radius of zinc ions leads to more difficult diffusion and larger de-solvation barriers. These two mechanisms usually work synergistically in zinc anode protection.

The organic small molecules strongly coordinate with Zn^{2+} and strong adsorb on the zinc anode. This results in a higher de-solvation polarization barrier, hindering the reduction process of Zn^{2+} and promoting nucleation rather than growth [44,82,85,98]. This can be manifested in higher polarization voltage and a more compact nucleation state, ultimately leading to long-lasting, uniform and smooth Zn stripping/plating interfaces. Polar small molecules can form hydrogen bonds with water molecules, resulting in the reduced activity of the water molecules. Therefore, they provide more feasibility for the design of low-temperature devices. Hao *et al.* proposed that typical monohydric alcohols, such as methanol, which can enter the inner solvation shell of Zn^{2+} due to their high dielectric constant and small size [99]. This alters the presence or arrangement of the six water molecules, resulting in uniform zinc deposition, inhibiting dendrite growth, and enhancing CE and cycle life. Ma *et al.* added isopropanol to maintain the $Zn(H_2O)_6{}^{2+}$ state and design the outer solvation shell of zinc ions (Fig. 6a), resulting in a smooth zinc deposition surface and higher CE [98]. This enabled a cycle life of over 2000 h for Zn/Zn symmetric batteries at −40 °C and over 1000 cycles for pouch batteries operated at −20 °C. Strong coordination with Zn^{2+} also implies a more challenging de-solvation polarization process, which prompt the introduction of weakly coordinating additives to facilitate the transition of Zn^{2+} from solvent structures dominated by water molecules to those dominated by anions [76]. Through the weak solvation effect, SEI derived from anions with high ion conductivity was constructed, providing a novel and effective strategy for electrolyte design. Polar small molecules may achieve dynamic adsorption of double layers during cycling, or form a stable SEI that stably controls Zn nucleation and growth (Fig. 6b), which is related to the composition design. Additionally, alcohol additives can lower the freezing point of the electrolyte [100], providing a low-cost and convenient approach for low-temperature aqueous batteries (Figs. 6c and d).

In addition to alcohol organic additives, other organic additives such as dimethyl sulfoxide (DMSO) [101,102], ethylenediaminetetraacetic acid (EDTA) [103], DMSO molecules with high donor number (DN) can tightly bind water molecules as hydrogen bond acceptors, reducing the number of free water molecules and enhancing the stability of the zinc anode. EDTA molecules, rich in polar functional groups such as O and F, chemically adsorb on the zinc anode surface, isolating water molecules and corrosion. By alternately combining electrochemical cycling and static resting, symmetric batteries achieved stable cycles of over 5000 h, providing effective improvement in the reversibility of zinc anodes under corrosion prevention strategies, supported by practical scientific validation. Moreover, succinonitrile (SN) [104], β-cyclodextrin (β-CD) [22], *N*,*N*-dimethyl acetamide (DMA) [77], 1,4-dioxane (DX) [85], γ-butyrolactone (GBL) [105], 1,3-benzenedisulfonic acid disodium salt (BSA) [106] and hexamethylenetetramine (HMTA) [79] have also been widely studied.

Organic polymers additives with long carbon chains, due to their excellent absorption characteristics, can inhibit the corrosion of zinc anode with only a small amount of addition. Li *et al.* used polymer PEG400 additives, and the polymer network adsorbed water molecules, significantly reducing the number of free water molecules at low salt concentrations (Fig. 6e) [107]. However, the abundance of functional groups in the polymer can lead to excessive chemical adsorption on the zinc surface, which sacrifices the kinetics of zinc ion deposition and dissolution, manifesting in the large polarization voltage. Moreover, as additives in aqueous electrolytes, the hydrophilicity of the polymer needs to be considered. The matching between the solubility and interface stability capability limited the organic polymer additives due to the long chain structure. Jin *et al.* introduced 0.5 wt% of long-chain polyethylene oxide (PEO) as an additive, where the electrochemically inert PEO molecules precisely adsorbed on the zinc anode surface, inhibiting hydrogen evolution corrosion [95]. The zinc anode exhibited stable cycles of over 3000 h (CE > 99.5%) (Figs. 6f and g). Xie *et al.* used water-soluble polymer polyethylene glycol (PEG) to broaden the operating voltage window (3.2 V) at low salt concentrations, providing insights for high-voltage aqueous batteries (Figs. 6h and i) [94].

3.4.2. Inorganic additives

Inorganic additives primarily include inorganic salts introduced as ion additives electrolyte concentration control agent [108–117]. These additives utilize dissolution equilibrium to introduce ions which are corresponding to the positive electrode. The pre-adding ions provide an advantageous recombination/dissolution equilibrium of cathodes, for example, $MgSO_4$ additives can reduce the dissolution of $Mg_xV_2O_5$ [113]. Moreover, the pre-adding ions can intercalate into cathodes along with the Zn^{2+}, thereby increasing capacity and inhibiting cathode dissolution, and other inorganic ions additives works with a similar mechanism (Figs. 6j and k) [109,110]. On the other hand, cations with a lower reduction potential than Zn^{2+}, produce an electrostatic shielding effect to suppress zinc dendrites *via* dynamic adsorption (Fig. 6l) [109]. Special anions mainly contribute to regulating the formation and component of SEI [118–120]. The inorganic non-metallic minerals [111], which can reduce the activity of water molecules and regulate the electrolyte concentration gradient, this is might an class of effective and low-cost additive and have certain research potential and gap for no-dendrite Zn anode.

In addition to the aforementioned control methods, there are also zinc salt anion design [121–123], pH regulation

Table 1
Summary of the cell performance of recently reported strategies developed for ZIBs.

Type	Electrolyte	Current density (mA/cm^2)	Capacity (mAh/cm^2)	Over-potential (mV)	Life-span (h)	CE (%)	Feature	Ref.
High-concentration electrolytes	1 mol/L $Zn(TFSI)_2$ + 20 mol/L liTFSI	0.2	0.034	150	170	99.7	Retains water in the open atmosphere	[49]
	4 mol/L $Zn(TFSI)_2$	0.25	0.25	40	700	97.5	\	[130]
	4 mol/L $Zn(SO)_4$	0.25	0.25	80	600	95.8	\	[130]
	30 mol/L ZnCl + 10 mol/L TMACl + 5 mol/L LiCl in H_2O/DMC (5:1)	1	1	40	260	99.95	Doublelayered inorganic–organic hybrid SEI	[48]
	7.5 mol/L $ZnCl_2$	0.2	0.2	25	400	97.93	Low-temperature aqueous batteries	[131]
	30 mol/L $ZnCl_2$	0.2	0.2	10	2000	99.03	\	[132]
	30 mol/L ZnCl + 5 mol/L LiCl	2	4	24	4000	99.7	\	[133]
	7.6 mol/L $ZnCl_2$ + 0.05 mol/L SnCl	3	3	20	500	99.7	Zincophilic and Zinophobic hybrid SEI	[134]
	1 mol/L $Zn(OTf)_2$ + 20 mol/L LiTFSI.	0.2	1	50	700	99.75	Anion-derived SEI	[135]
Ionic liquids	0.1 mol/L ImS + $ZnSO_4$	1	1	90	3400	99.9	\	[27]
	EmimFSI + $Zn(OTf)_2$	1	1	100	690	~99	\	[28]
	BMImOTf + $ZnSO_4$	2	1	100	3300	99.8	Preference growth of Zn (002)	[59]
	BMITFSI + $Zn(TFSI)_2$	1	0.5	100	1000	99.27	Inorganic–organic complex SEI	[56]
	[BMIm]OTf + $Zn(OTf)_2$	1	1	50	1000	99.46	Inorganic–organic complex SEI	[55]
	Imidazole + $ZnCl_2$	1	1	30	240	\	\	[54]
	$[EMIM]BF_4$ + $Zn(BF_4)_2$	2	1	75	1500	99.36	Ionic-liquid-based all-solid-state Zn-ion battery Ionic conductivity of 1.69×10^{-2} S/cm	[57]
	[Emim]OTf + PEO polymer + ZnO nanofillers	0.1	0.1	150	1800	\	Ionic conductivity of 0.23×10^{-2} S/cm	[58]
Gel-polymer electrolyte	PAM/PPF-SSEs + $Zn(OTF)_2$	2	4	30	2000	99.9	Ionic conductivity of 5.086×10^{-4} S/cm	[61]
	Pseudopolyrotaxane gel electrolyte	0.7	0.7	80	1300	~100	Ionic conductivity of 0.8×10^{-2} S/cm	[32]
	PAAM + Chitosan + $Zn(OTf)_2$	0.5		90	370	99.02	Ionic conductivity of 1.16×10^{-2} S/cm	[34]
	Xanthan bio-polymer + $ZnSO_4$ + $MnSO_4$	\		\	\	\	Ionic conductivity of 1.46×10^{-2} S/cm	[136]
	Acid PAM hydrogel + Alkaline PAA-Na + Neutral PAM + $ZnSO_4$	\		\	\	\	Ionic conductivity of 1.463×10^{-2} S/cm	[73]
	PVA + $Zn(OTf)_2$	0.1	0.1	85	800		Ionic conductivity of 1.5×10^{-2} S/cm	[53]
	Alginate polymer	5	1.25	100	500	99.65	Ionic conductivity of 2.5×10^{-2} S/cm	[49]
	Tannic acid + Sodium alginate + $ZnSO_4$	1.13	0.2825	50	300	~100	Ionic conductivity of 2.42×10^{-2} S/cm	[48]
	PSBMA polymer + $ZnSO_4$	1		150	1900	\	Ionic conductivity of 3.20×10^{-2} S/cm	[47]
	Palygorskite + Sodium alginate + $ZnSO_4$ + Na_2SO_4	1	0.48	50	600	\	\	[57]
Additive electrolyte	Methanol + $ZnSO_4$	1	0.5	\	\	99.7	\	[78]
	Ethanol+ $Zn(OTf)_2$ + NaOTf	0.5	0.5	50	670	99.7	\	[25]
	Ethylene glycol + $ZnSO_4$	2	1	60	150	94	High zinc-ion conductivity (6.9 mS/cm at −40 °C)	[79]
	2-Propanol + $Zn(OTf)_2$	1	1	100	3000	99.06	Regulation of outer solvation shell	[98]
		15	15	200	500	\		
	Tripropylene glycol + $ZnSO_4$	1	0.5	180	1100	99.73	\	[82]
	Sorbitol + $ZnSO_4$	1	1	50	1200	96.9	\	[137]
	2,2,2-Trifluoroethanol + $ZnCl_2$	0.2	0.2	8	4000	99.74	Smaller Zn^{2+} solvation clusters	[132]
	Ethylene glycol monomethyl ether + $ZnSO_4$	1	0.5	100	8000	99.5	\	[138]
	γ-Butyrolactone + $ZnSO_4$	2	1	50	5000	98.6	\	[105]
	Sac+ $ZnSO_4$	0.5	0.5	60	500	\	\	[80]
		10	10	80	550	99.6		
	1,4-Dioxane + $ZnSO_4$	1	1	100	1200	99.7	Exposure of Zn (002) facets	[85]
	1,4-Dioxane + $Zn(OTf)_2$ + NaOTf	0.5	2	60	5000	99.0	Weakly solvating effect Inorganic SEI	[76]
	Succinonitrile + $ZnSO_4$	1	2	100	700	99.71	Zincophobic electrolyte and horizontal stacking of SEI	[104]
	Glycine + $ZnSO_4$	1	1	50	3200	99.68	ZnS-rich SEI layer	[86]
	NH_4Ac + $ZnSO_4$	2	2	80	500	99.50	CF/CF_3-rich SEI and stabler PH	[119]
	N,*N*-Dimethylformamidium trifluoromethanesulfonate + $ZnSO_4$	4	4	60	350	99.97	Nanostructured SEI	[120]
	N,*N*-Dimethyl acetamide + $ZnSO_4$	1	0.5	100	4500	99.60	\	[77]
	Zinc formate + $ZnSO_4$	5	1	80	2400	99.80	Stabler PH	[81]
	Sericin molecules + $ZnSO_4$	1	1	100	4400	99.29	Insulating SEI	[44]
	Urea + LiOAc + $Zn(OTf)_2$	4.8	1	30	600	99.7	Hybrid solute additives	[39]
	Polyethylene oxide polymer + $ZnSO_4$	\		\	\	99.5	\	[95]
	Polyethylene glycol 400 + $Zn(OTf)_2$	0.5	1	220	1800	99.7	\	[107]
	$La(NO_3)_3$ + $ZnSO_4$	1	1	40	1200	99.9	\	[108]

[73,81,118,119,124], electrochemical methods [125–127] and flow batteries [128,129]. Furthermore, zinc-ion batteries have also achieved certain achievements in non-aqueous electrolyte field [53], but it is beyond the scope of this article and will not be elaborated.

4. Conclusion and perspectives

In summary, the instability of the zinc anode in the electrolyte is caused by the polarization of active water molecules on the zinc anode surface, resulting in issues such as zinc dendrites, hydrogen evolution corrosion, byproduct formation, and passivation. These problems are mutually reinforcing, leading to a vicious cycle and severe deterioration of the performance of aqueous zinc-ion batteries. To control the polarization of active water molecules on the zinc metal surface, effective strategies in electrolyte regulation engineering include: (1) Eliminating water from the solvation shell of Zn^{2+}; (2) forming hydrophobic films on the zinc anode surface; (3) designing stable SEI structures to block protons from reaching the zinc surface; and (4) inducing the texture growth of Zn (002). To sum up, a number of recently reported water molecules regulation strategies are shown in Table 1 [25,27,28,32,34,39,44,47–49,53–59,61,73,76–78,80–82,85,86,95,98,104,105,107,108,119,120,130–138].

Specific electrolyte regulation engineering approaches to implement the aforementioned strategies include:

(1) Reducing the water content in the electrolyte, such as using high-concentration electrolytes, ionic liquids, and gel polymer electrolytes. While high-concentration electrolytes and ionic liquids widen the electrochemical window and offer excellent electrochemical performance, their high cost hinders industrial applications. Gel polymer electrolytes provide good mechanical properties and high safety, opening up new possibilities for biological application. However, their electrochemical performance is limited by the low ion conductivity.

(2) Isolating the water molecules from the Zn anode. For instance, functional additives preferentially adsorb onto the zinc anode surface, forming a dynamic hydrophobic film. Moreover, the similar positive effects act on the cathode. The adsorption of polar induced molecules on the electrode surface is not enough to form a strong protective layer to enhance the stability of the two electrodes. It is possible to achieve the *in-situ* formation of hydrophobic but zinc-philic SEI on the Zn anode surface due to the preferential electroreduction of added ingredients. However, low-cost additives that can take effect by micro-addition are necessary.

(3) Regulating the activity of water molecules. Functional additives form hydrogen bonds with water molecules to suppress polarization, and enhance the electrochemical performance under low temperature. The stronger binding energy with Zn^{2+} than water molecules lead to expel water content from the solvation structure of Zn^{2+}, thus settling the parasitic side reactions. Functional additives with excellent effects are simple to apply, making them crucial in optimizing the industrialization of aqueous zinc-ion batteries.

For practical AZIBs, there are also demands for high electric conductivity gel-polymer electrolytes and low-cost high-concentration additives. Development of more ionic liquids is worthwhile after in-depth understanding of the role of anions and cations. Organic additives with polar functional groups (such as F, O, S, and N) are widely studied, organic molecules with the polar functional groups including -CF_3, -phenyl are worthwhile to research in AZIBs. To sum up, the general trend is that the stronger the polarity, the tighter the adsorption on the zinc anode surface to exclude water molecules. However, there is still a lack of descriptors that accurately describe the relationship among polar functional groups, water molecules zinc ions, and anion. Most functional additives are determined through empirical and experimental trial-and-error methods, considering parameters like viscosity, steric hindrance, and dielectric constants. It is crucial to design functional additives to regulate the solvation structure of Zn^{2+} while reducing the barrier of de-solvation, appropriate descriptors

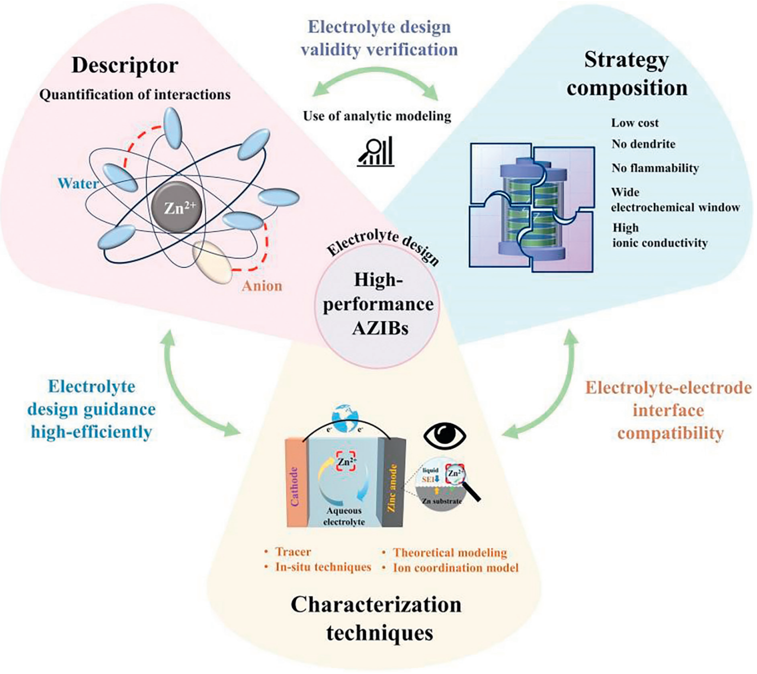

Fig. 7. Schematic diagram of future electrolyte engineering prospects for high-performance AZIBs.

are necessary, closely relating to solvation structures, to guide the molecular design of additives at a fundamental level. Regarding the extent of changes in the solvation structure of zinc ions and the diffusion behaviors of zinc ions through the formed SEI, there is still unclear, and the research on electrochemical stripping are deficient. These issues may be improved through the continuous development of experimental and computational models and *in-situ* characterization techniques. Otherwise, for high performance AZIBs, the engineering of composite electrolytes combining various strategies can lead to synergistic effects, which can match various demand in energy storage (Fig. 7).

Declaration of competing interest

There are no conflicts of interest to declare.

Acknowledgments

This research was financially supported by the Science Fund for Natural Science Foundation of Hunan Province (No. 2023JJ20064), the National Natural Science Foundation of China (No. 52377222) and Natural Science Foundation of Hunan Province (No. 2023JJ50012).

References

[1] Z. Piao, R. Gao, Y. Liu, et al., Adv. Mater. 35 (2023) 2206009.
[2] Q. Zhang, X. Zhang, J. Wan, et al., Nat. Energy 8 (2023) 725–735.
[3] C. Yan, H. Li, X. Chen, et al., J. Am. Chem. Soc. 141 (2019) 9422–9429.
[4] K. Long, S. Huang, H. Wang, et al., Energy Storage Mater. 58 (2023) 142–154.
[5] J. Yang, R. Zhao, Y. Wang, et al., Adv. Funct. Mater. 33 (2023) 2370084.
[6] Q. Li, H. Wang, H. Yu, et al., Adv. Funct. Mater. 33 (2023) 2303466.
[7] Y. Liang, Y. Yao, Nat. Rev. Mater. 8 (2022) 109–122.
[8] X. Yu, Z. Li, X. Wu, et al., Joule 7 (2023) 1145–1175.
[9] H. Li, S. Guo, H. Zhou, Energy Storage Mater. 56 (2023) 227–257.
[10] Y. Zhu, Y. Cui, Z. Xie, et al., Nat. Rev. Chem. 6 (2022) 505–517.
[11] X. Li, X. Wang, L. Ma, et al., Adv. Energy Mater. 12 (2022) 2202068.
[12] S. Guo, L. Qin, T. Zhang, et al., Energy Storage Mater. 34 (2021) 545–562.
[13] J. Song, K. Xu, N. Liu, et al., Mater. Today 45 (2021) 191–212.
[14] D. Wang, Q. Li, Y. Zhao, et al., Adv. Energy Mater. 12 (2022) 2102707.
[15] L. Miao, Z. Guo, L. Jiao, Energy Mater. 3 (2023) 300014.
[16] J. Yin, X. Feng, Z. Gan, et al., Energy Storage Mater. 54 (2023) 623–640.
[17] M. Li, Z. Li, X. Wang, et al., Energy Environ. Sci. 14 (2021) 3796–3839.
[18] O. Borodin, J. Self, K.A. Persson, et al., Joule 4 (2020) 69–100.
[19] Z. Li, A.W. Robertson, Battery Energy 2 (2023) 20220029.
[20] W. Yang, Y. Yang, H. Yang, et al., ACS Energy Lett. 7 (2022) 2515–2530.
[21] Y. He, Y. Cui, W. Shang, et al., Chem. Eng. J. 438 (2022) 135541.
[22] C. Meng, W. He, L. Jiang, et al., Adv. Funct. Mater. 32 (2022) 2207732.
[23] Z. Zhao, J. Zhao, Z. Hu, et al., Energy Environ. Sci. 12 (2019) 1938–1949.
[24] Y. Zhao, C. Yang, Y. Yu, Chin. Chem. Lett. 35 (2024) 108865.
[25] N. Zhang, F. Cheng, Y. Liu, et al., J. Am. Chem. Soc. 138 (2016) 12894–12901.
[26] S. Cai, X. Chu, C. Liu, et al., Adv. Mater. 33 (2021) 2007470.
[27] Y. Lv, M. Zhao, Y. Du, et al., Energy Environ. Sci. 15 (2022) 4748–4760.
[28] L. Yu, J. Huang, S. Wang, et al., Adv. Mater. 35 (2023) 2210789.
[29] M. Xu, D.G. Ivey, W. Qu, et al., J. Power Sources. 274 (2015) 1249–1253.
[30] S. Sen, S.E. Goodwin, P.V. Barbará, et al., ACS Appl. Polym. Mater. 3 (2021) 200–208.
[31] K. Wu, J. Cui, J. Yi, et al., ACS Appl. Mater. Interfaces 14 (2022) 34612–34619.
[32] K. Wu, S. Zhan, W. Liu, et al., ACS Appl. Mater. Interfaces 15 (2023) 6839–6847.
[33] Z. Xu, Z. Zhang, X. Li, et al., ACS Appl. Mater. Interfaces 15 (2023) 15574–15584.
[34] Y. Liu, A. Gao, J. Hao, et al., Chem. Eng. J. 452 (2023) 139605.
[35] H. Li, Z. Liu, G. Liang, et al., ACS Nano 12 (2018) 3140–3148.
[36] S. Lv, T. Fang, Z. Ding, et al., ACS Nano 16 (2022) 20389–20399.
[37] X. Xu, Y. Xu, J. Zhang, et al., Nano Micro Lett. 15 (2023) 56.
[38] J. Cao, D. Zhang, X. Zhang, et al., Energy Environ. Sci. 15 (2022) 499–528.
[39] X. Feng, P. Li, J. Yin, et al., ACS Energy Lett. 8 (2023) 1192–1200.
[40] A. Bayaguud, X. Luo, Y. Fu, et al., ACS Energy Lett. 5 (2020) 3012–3020.
[41] Y. Sun, Z. Xu, X. Xu, et al., Energy Storage Mater. 48 (2022) 192–204.
[42] Y. Shang, P. Kumar, U. Mittal, et al., Energy Storage Mater. 55 (2023) 117–129.
[43] H. Huang, J. Yun, H. Feng, et al., Energy Storage Mater. 55 (2023) 857–866.
[44] H. Wang, H. Li, Y. Tang, et al., Adv. Funct. Mater. 32 (2022) 2207898.
[45] T. Wen, B. Qu, S. Tan, et al., Energy Storage Mater. 55 (2023) 816–825.
[46] M. Li, G. Lu, W. Zheng, et al., Adv. Funct. Mater. 33 (2023) 2214759.
[47] F. Wan, Y. Zhang, L. Zhang, et al., Angew. Chem. Int. Ed. 58 (2019) 7062–7067.
[48] H. Jiang, L. Tang, Y. Fu, et al., Nat. Sustain. 6 (2023) 806–815.
[49] F. Wang, O. Borodin, T. Gao, et al., Nat. Mater. 17 (2018) 543–549.
[50] H. Lu, D. Zhang, Q. Jin, et al., Adv. Mater. 35 (2023) 2300620.
[51] J. Wang, J. Tian, G. Liu, et al., Small Methods 7 (2023) 2300392.
[52] R.D. Rogers, K.R. Seddon, Science 302 (2003) 792–793.
[53] Y. Lv, Y. Xiao, L. Ma, et al., Adv. Mater. 34 (2022) 2106409.
[54] A. Rana, A. Thakare, N. Kumar, et al., ACS Appl. Mater. Interfaces 15 (2023) 23093–23103.
[55] J. Chen, W. Zhou, Y. Quan, et al., Energy Storage Mater. 53 (2022) 629–637.
[56] Z. Zhao, J. Lai, D.T. Ho, et al., ACS Energy Lett. 8 (2023) 608–618.
[57] L. Ma, S. Chen, N. Li, et al., Adv. Mater. 32 (2020) 1908121.
[58] D. Wang, X. Guo, Z. Chen, et al., ACS Appl. Mater. Interfaces 14 (2022) 27287–27293.
[59] H. Zhang, Y. Zhong, J. Li, et al., Adv. Energy Mater. 13 (2023) 2203254.
[60] X. Lang, Z. Hu, C. Wang, Chin. Chem. Lett. 32 (2021) 999–1009.
[61] S. Chen, Y. Ying, L. Ma, et al., Nat. Commun. 14 (2023) 2925.
[62] C. Han, W. Li, H.K. Liu, et al., Nano Energy 74 (2020) 104880.
[63] J. Fu, D.U. Lee, F.M. Hassan, et al., Adv. Mater. 27 (2015) 5617–5622.
[64] K. Leng, G. Li, J. Guo, et al., Adv. Funct. Mater. 30 (2020) 2001317.
[65] B. Zhang, L. Qin, Y. Fang, et al., Sci. Bull. 67 (2022) 955–962.
[66] W. Yang, X. Du, J. Zhao, et al., Joule 4 (2020) 1557–1574.
[67] X. Xie, J. Li, Z. Xing, et al., Natl. Sci. Rev. 10 (2023) nwac281.
[68] C. Li, X. Xie, H. Liu, et al., Natl. Sci. Rev. 9 (2022) nwab177.
[69] S.N. Banitaba, D. Semnani, E. Heydari-Soureshjani, et al., Mater. Res. Express 6 (2019) 0850d6.
[70] W. Prasadini, K.S. Perera, K.P. Vidanapathirana, et al., AIMS Energy 6 (2018) 566–575.
[71] Z. Shen, J. Mao, G. Yu, et al., Angew. Chem. Int. Ed. 62 (2023) e202218452.
[72] S. Huang, F. Wan, S. Bi, et al., Angew. Chem. Int. Ed. 58 (2019) 4313–4317.
[73] Z. Shen, Z. Tang, C. Li, et al., Adv. Energy Mater. 11 (2021) 2102055.
[74] A.M. Hyde, S.L. Zultanski, J.H. Waldman, et al., Org. Process Res. Dev. 21 (2017) 1355–1370.
[75] W. Yu, J. Ge, Y. Hu, et al., Sci. China Mater. 66 (2023) 923–931.
[76] Y. Yang, G. Qu, H. Wei, et al., Adv. Energy Mater. 13 (2023) 2203729.
[77] W. Deng, Z. Xu, X. Wang, Energy Storage Mater. 52 (2022) 52–60.
[78] M. Yan, C. Xu, Y. Sun, et al., Nano Energy 82 (2021) 105739.
[79] H. Yu, D. Chen, Q. Li, et al., Adv. Energy Mater. 13 (2023) 2300550.
[80] C. Huang, X. Zhao, S. Liu, et al., Adv. Mater. 33 (2021) 2100445.
[81] Y. Gao, M. Wang, H. Wang, et al., J. Energy Chem. 84 (2023) 62–72.
[82] Z. Liu, R. Wang, Q. Ma, et al., Adv. Funct. Mater. 33 (2023) 2214538.
[83] R. Qin, Y. Wang, M. Zhang, et al., Nano Energy 80 (2021) 105478.
[84] Z. Miao, Q. Liu, W. Wei, et al., Nano Energy 97 (2022) 107145.
[85] T. Wei, Y. Ren, Y. Wang, et al., ACS Nano 17 (2023) 3765–3775.
[86] Y. Liu, Y. An, L. Wu, et al., ACS Nano 17 (2023) 552–560.
[87] N. Wang, Y. Yang, X. Qiu, et al., ChemSusChem 13 (2020) 5556–5564.
[88] J. Lee, B. Hwang, M.-S. Park, et al., Electrochim. Acta 199 (2016) 164–171.
[89] S. Hosseini, S.J. Han, A. Arponwichanop, et al., Sci. Rep. 8 (2018) 11273.
[90] C. Han, Y. Yao, S. Lv, et al., Optik (Stuttg) 155 (2018) 307–314.
[91] P. Sun, L. Ma, W. Zhou, et al., Angew. Chem. 133 (2021) 18395–18403.
[92] M. Liang, H. Zhou, Q. Huang, et al., J. Appl. Electrochem. 41 (2011) 991–997.
[93] B. Liu, T. Wu, F. Ma, et al., ACS Appl. Mater. Interfaces 14 (2022) 18431–18438.
[94] J. Xie, Z. Liang, Y.C. Lu, Nat. Mater. 19 (2020) 1006–1011.
[95] Y. Jin, K.S. Han, Y. Shao, et al., Adv. Funct. Mater. 30 (2020) 2003932.
[96] V.K. Nartey, L. Binder, K. Kordesch, J. Power Sources 52 (1994) 217–222.
[97] H. Zhou, Q. Huang, M. Liang, et al., Mater. Chem. Phys. 128 (2011) 214–219.
[98] Q. Ma, R. Gao, Y. Liu, et al., Adv. Mater. 34 (2022) 2207344.
[99] J. Hao, L. Yuan, C. Ye, et al., Angew. Chem. Int. Ed. 60 (2021) 7366–7375.
[100] N. Chang, T. Li, R. Li, et al., Energy Environ. Sci. 13 (2020) 3527–3535.
[101] Q. Nian, X. Zhang, Y. Feng, et al., ACS Energy Lett. 6 (2021) 2174–2180.
[102] L. Cao, D. Li, E. Hu, et al., J. Am. Chem. Soc. 142 (2020) 21404–21409.
[103] Y. Ou, Z. Cai, J. Wang, et al., EcoMat 4 (2022) e12167.
[104] N. Wang, X. Chen, H. Wan, et al., Adv. Funct. Mater. 33 (2023) 2300795.
[105] P. Xiao, Y. Wu, J. Fu, et al., ACS Energy Lett. 8 (2023) 31–39.
[106] X. Gan, J. Tang, X. Wang, et al., Energy Storage Mater. 59 (2023) 102769.
[107] C. Li, R. Kingsbury, L. Zhou, et al., ACS Energy Lett. 7 (2022) 533–540.
[108] R. Zhao, H. Wang, H. Du, et al., Nat. Commun. 13 (2022) 3252.
[109] F. Wan, L. Zhang, X. Dai, et al., Nat. Commun. 9 (2018) 1656.
[110] H. Tian, G. Feng, Q. Wang, et al., Nat. Commun. 13 (2022) 7922.
[111] L. Yang, T. Zhang, S. Liu, et al., Small Methods (2023), doi:10.1002/smtd.202300009.
[112] H. Guo, Z. Shao, Y. Zhang, et al., J. Colloid Interface Sci. 608 (2022) 1481–1488.
[113] Y. Zhang, H. Li, S. Huang, et al., Nano-Micro Lett. 12 (2020) 60.
[114] V. Soundharrajan, B. Sambandam, S. Kim, et al., Energy Storage Mater. 28 (2020) 407–417.
[115] H.Y. Wu, X. Gu, P. Huang, et al., J. Mater. Chem. A 9 (2021) 7025–7033.
[116] C. Yang, J. Xia, C. Cui, et al., Nat. Sustain. 6 (2023) 325–335.
[117] H. Wang, A. Zhou, X. Hu, et al., ACS Nano 17 (2023) 11946–11956.
[118] R. Chen, W. Zhang, Q. Huang, et al., Nano-Micro Lett. 15 (2023) 81-81.
[119] X. Zhao, N. Dong, M. Yan, et al., ACS Appl. Mater. Interfaces 15 (2023) 4053–4060.
[120] C. Li, A. Shyamsunder, A.G. Hoane, et al., Joule 6 (2022) 1103–1120.
[121] H. Du, Y. Dong, Q. Li, et al., Adv. Mater. 35 (2023) 2210055.
[122] X. Xu, H. Su, J. Zhang, et al., ACS Energy Lett. 7 (2022) 4459–4468.
[123] X. Zeng, J. Liu, J. Mao, et al., Adv. Energy Mater. 10 (2020) 1904163.
[124] S.J. Zhang, J. Hao, Y. Zhu, et al., Angew. Chem. Int. Ed. 62 (2023) e202301570.
[125] C.J. Lan, C.Y. Lee, T.S. Chin, Electrochim. Acta 52 (2007) 5407–5416.
[126] A. Pei, G. Zheng, F. Shi, et al., Nano Lett. 17 (2017) 1132–1139.
[127] W. Yuan, X. Nie, G. Ma, et al., Angew. Chem. Int. Ed. 62 (2023) e202218386.
[128] J. Yang, H. Yan, H. Hao, et al., ACS Energy Lett. 7 (2022) 2331–2339.

[129] X. Fan, X. Ji, L. Chen, et al., Nat. Energy. 4 (2019) 882–890.
[130] N. Patil, C. Cruz, D. Ciurduc, et al., Adv. Energy Mater. 11 (2021) 2100939.
[131] Q. Zhang, Y. Ma, Y. Lu, et al., Nat. Commun. 11 (2020) 4463.
[132] R. Wang, M. Yao, M. Yang, et al., Proc. Natl. Acad. Sci. U. S. A. 120 (2023) e2221980120.
[133] C. Zhang, W. Shin, L. Zhu, et al., Carbon Energy 3 (2021) 339–348.
[134] L. Cao, D. Li, F.A. Soto, et al., Angew. Chem. Int. Ed. 60 (2021) 18845–18851.
[135] A. Clarisza, H.K. Bezabh, S.K. Jiang, et al., ACS Appl. Mater. Interfaces 14 (2022) 36644–36655.
[136] S. Zhang, N. Yu, S. Zeng, et al., J. Mater. Chem. A 6 (2018) 12237–12243.
[137] M. Qiu, P. Sun, A. Qin, et al., Energy Storage Mater. 49 (2022) 463–470.
[138] M. Liu, L. Yao, Y. Ji, et al., Nano Lett. 23 (2023) 541–549.